



PAPER • OPEN ACCESS

Folic acid-decorated vitamin E Poly(ethylene glycol) monoplatinum ester with disulfide bond as theranostic nanoparticle for drug resistant tumor diagnosis and treatment

To cite this article: Zhuoran Li *et al* 2023 *Mater. Res. Express* **10** 115404

View the [article online](#) for updates and enhancements.

You may also like

- [Apoptosis induced by paclitaxel-loaded copolymer PLA-TPGS in Hep-G2 cells](#)
Hoai Nam Nguyen, Hong Ha Tran Thi, Duong Le Quang *et al.*
- [Lactobionic acid-conjugated TPGS nanoparticles for enhancing therapeutic efficacy of etoposide against hepatocellular carcinoma](#)
Altansukh Tsend-Ayush, Xiumei Zhu, Yu Ding *et al.*
- [Alpha-tocopheryl polyethylene glycol succinate-emulsified poly\(lactic-co-glycolic acid\) nanoparticles for reversal of multidrug resistance *in vitro*](#)
Ying Wang, Miao Guo, Yu Lu *et al.*

ECS
The
Electrochemical
Society
Advancing solid state &
electrochemical science & technology

DISCOVER
how sustainability
intersects with
electrochemistry & solid
state science research



PAPER

OPEN ACCESS

RECEIVED
29 June 2023REVISED
1 November 2023ACCEPTED FOR PUBLICATION
15 November 2023PUBLISHED
30 November 2023

Original content from this work may be used under the terms of the Creative Commons Attribution 4.0 licence.

Any further distribution of this work must maintain attribution to the author(s) and the title of the work, journal citation and DOI.



Folic acid-decorated vitamin E Poly(ethylene glycol) monoplatinum ester with disulfide bond as theranostic nanoparticle for drug resistant tumor diagnosis and treatment

Zhuoran Li^{1,5} , Huikang Yang^{2,5}, Fan Xu^{1,5}, Xuwen Zeng^{1,*}, Haowei Huang^{3,*} and Xinqing Jiang^{2,4,*}

- ¹ Department of Radiology, Guangzhou Red Cross Hospital of Jinan University, Guangzhou, Guangdong, People's Republic of China
² Department of Radiology, Guangzhou First People's Hospital, School of Medicine, South China University of Technology, Guangzhou, Guangdong, People's Republic of China
³ Department of Radiotherapy, Guangzhou Red Cross Hospital of Jinan University, Guangzhou, Guangdong, People's Republic of China
⁴ Department of Radiology, Guangzhou First People's Hospital, Jinan University, Guangzhou, Guangdong, People's Republic of China
⁵ These authors contributed equally to this work and share first authorship.
* Authors to whom any correspondence should be addressed.

E-mail: lizr2023@qq.com, gzhshzhyfysk@163.com, hwh522@qq.com and eyjiangxq@scut.edu.cn**Keywords:** multidrug resistance, TPGS, tumor-targeted, disulfide bond, theranostic nanoparticles

Abstract

Vitamin E Poly(ethylene glycol) monoplatinum ester (TPGS) nanoparticles have attracted much attention in recent years for overcome multidrug resistance. Herein, a well-defined folic acid (FA)-conjugated and disulfide bond-linked polymer (FA-SS-TPGS) was synthesized. These polymer nanoparticles were utilized as theranostic agents for tumor-targeted magnetic resonance imaging (MRI) and chemotherapy. By loading doxorubicin (DOX) and superparamagnetic iron oxide (SPIO) particles into TPGS nanoparticles, FA-SS-TPGS@DOX/SPIO nanoparticles are obtained. *In vitro* drug release studies revealed that under a reducing environment in the presence of glutathione (GSH), approximately 100% of the doxorubicin (DOX) was released from the disulfide bond-linked theranostic nanoparticles within 24 h. DOX and SPIO were efficiently delivered into HepG2-ADM cells due to the folate receptor-mediated endocytosis process of the nanoparticles. Additionally, the presence of glutathione (GSH) triggered the cleaving of the disulfide bonds, further facilitating the delivery of DOX and SPIO into the cells. Furthermore, the FA-SS-TPGS@DOX-SPIO nanoparticles exhibited strong MRI contrast enhancement properties. In conclusion, FA-SS-TPGS@DOX/SPIO are potential nanoparticles for tumor-targeted MRI and chemotherapy, which can also overcome multidrug resistance.

1. Introduction

Multiple-drug resistance (MDR) poses a significant challenge in tumor chemotherapy, as it significantly limits the effectiveness of chemotherapy in killing tumor cells. This presents a major problem for clinicians seeking to cure patients [1, 2]. Numerous studies have focused on finding solutions to overcome multidrug resistance. Some common approaches involve prolonging drug circulation time, enhancing cell-specific or tissue-specific targeting, and reducing systemic side effects. These strategies aim to improve the therapeutic efficacy of chemotherapy while minimizing its adverse effects [3–7].

Nanotechnology has made rapid progress in the treatment of tumors and is gradually showing its potential [8, 9]. Nanotechnology can deliver chemotherapeutic drugs to target cells more accurately by encapsulating or binding them to nanocarriers, which provides new ideas and prospects for avoiding multidrug resistance [10]. Tocopheryl Poly(ethylene glycol) succinate (TPGS) is a vitamin E-related derivative, which is esterified by vitamin E succinate carboxyl and Poly(ethylene glycol). TPGS acts as an excellent surfactant and, when polymerized into micelles with drugs, can improve the absorption rate in the gastrointestinal tract, thus significantly enhancing drug utilization [11–13]. Moreover, TPGS nanoparticles exhibit increased drug

encapsulation efficiency, facilitate the uptake of chemotherapy drugs by cells, prolong blood circulation time, and enhance the bioavailability of anticancer drugs [14, 15]. Due to its tocopherol ester structure, TPGS also possesses antioxidant properties, making it more stable than other preparations. Owing to the pH sensitivity, TPGS nanoparticles showed higher targeting for tumor cells [16]. And the nano-drug delivery system, such as liposomes, micelles, and nano-particles, stands out due to the better outcomes of tumor-targeting, anti-tumor activities, immune-sensitization, stability, and safety [17]. Consequently, synthesizing TPGS-based nanoparticles improves the absorption and cellular uptake of anticancer drugs, enhancing drug utilization and therapeutic effectiveness [11, 18].

Environmentally responsive polymer materials can play a crucial role in controlling drug release and enhancing the efficiency and effectiveness of drug delivery. Disulfide bonds (-SS-) are known to be stable under normal physiological conditions, such as body temperature and pH. However, they can be easily reduced and broken in the presence of glutathione (GSH) [19]. GSH is abundant in cells and serves as an intracellular reducing agent. By incorporating disulfide bonds into polymer nanoparticles, drug release can be triggered in a controlled manner by taking advantage of the high GSH levels found within cells. Many studies have shown that doxorubicin can be rapidly released under acidic conditions. This is mainly due to the fact that doxorubicin is a hydrophobic molecule with a monoamino group. Under acidic conditions, the amino group of doxorubicin becomes protonated, resulting in the formation of a more water-soluble doxorubicin amino salt, such as doxorubicin hydrochloride. The increased solubility of doxorubicin hydrochloride under acidic conditions leads to the rapid release of the drug from drug delivery systems, which can enhance the therapeutic efficacy in tumor microenvironments with low pH levels [20]. This allows for site-specific drug release and improved therapeutic outcomes.

Folic acid has been widely used as a targeting ligand for tumor drug therapy. The effectiveness of folic acid conjugated drugs mainly depends on the presence of folate receptors (FRs) on the surface of target cells. FRs are overexpressed on many tumor cells, including hepatocellular carcinoma (HCC) cells, compared to normal cells [21]. There is a lot of literature linking FA to the hydrophilic end of PEG. The introduction of folic acid has shown an increase in the uptake capacity of tumor cells and an improved inhibitory effect of drugs on tumor cell growth [22]. Therefore, nanoparticles conjugated with folic acid can specifically target and deliver drugs to HCC cells. This approach improves the therapeutic efficacy and reduces systemic side effects, making it a promising strategy for targeted drug delivery in cancer therapy [23].

Superparamagnetic iron oxide (SPIO) nanoparticles are commonly used in negative contrast agents for magnetic resonance imaging (MRI) due to their high safety and higher contrast ratio compared to traditional contrast agents [24, 25]. These particles can shorten the transverse relaxation rate and improve image quality. They can also be used in drug therapy and controlled under magnetic resonance imaging guidance, allowing for targeted tumor therapy [26]. In addition, Iron oxide nanoparticles, specifically SPIONs, exhibit low toxicity in humans. Hence, SPIONs have received approval for use as contrast imaging agents in MRI due to their high safety factor. In contrast with other metal oxide nanoparticles, iron oxide nanoparticles demonstrate superior drug safety and no cytotoxicity at mass concentrations less than $100 \mu\text{g ml}^{-1}$ [27].

Regarding DOX-loaded TPGS micelles, a systematic evaluation was performed at the cellular level to investigate their ability to reverse multidrug resistance (MDR) mechanisms. TPGS micelles have shown promise in overcoming MDR due to their ability to enhance drug uptake, prolong blood circulation time, and improve the bioavailability of anticancer drugs. By encapsulating DOX into TPGS micelles, drug resistance mechanisms can be reversed at the cellular level, resulting in improved therapeutic efficacy [28]. The investigation focused on developing a drug delivery system called FA-SS-TPGS@DOX/SPIO nanoparticles, specifically designed to overcome multidrug resistance (MDR). The nanoparticles were fabricated by loading DOX into the nanoparticles using the dialysis method. The cytotoxicity of these DOX-loaded nanoparticles was then evaluated against HepG2-ADM, and the mechanism for overcoming MDR was studied.

2. Materials and methods

2.1. Materials

N,N-dimethylformamide (DMF, 99.5%) was purchased from the Chemical Reagent Sinopharm Group. Folic acid (FA, 99%), allyl PGE 1000, doxorubicin hydrochloride (DOX.HCl); glutathione (GSH), ferric acetyl acetate (III, 99%), D- α -tocopherol succinate (99%), vitamin E Poly(ethylene glycol) monoplatinum ester (TPGS), and N,N'-carbonyl diimidazole (CDI) were acquired from Aladdin Chemical Company (Shanghai, China). Sodium ascorbate (99%), copper sulfate ($\text{CuSO}_4 \cdot 5\text{H}_2\text{O}$, 95%), and Doxorubicin hydrochloride (99%) were acquired from Alfa Aesar. Tetrahydrofuran (THF) was purchased from Guangzhou Jianhua Biological Technology Company. Dulbecco's modified Eagle medium (DMEM), trypsin-ethylenediaminetetraacetic acid (trypsin-EDTA), Penicillin streptomycin, and fetal bovine serum (FBS) were purchased from Gibco-BRL

(Melbourne, Australia). Prussian blue stain (for cells) was purchased from Beijing Regen Biological Company, and 4,6-Diamidino-2-phenylindole (DAPI) was purchased from Beyotime Institute of Biotechnology (Nanjing, China). CCK-8 kit was purchased from MedChemExpress. Calcein-AM/PI double dye reagent was purchased from Shenzhen Xinbosheng Company.

2.2. Synthesis of FA-SS-TPGS

Briefly, 10 g of allyl Poly(ethylene glycol) 1000 was added into a 250 ml round-bottom flask, and then 100 ml anhydrous dichloromethane was added and dissolved while stirring in an ice water bath. Furthermore, 2 g p-methylbenzene sulfonyl chloride was added along with 3 ml triethylamine, and was continued to stir for 2 h, leaving it to stir continuously for the next 24 h. The organic phase was washed three times with saturated sodium bicarbonate solution and then separated to obtain the organic phase. The dichloromethane was removed by pressure distillation, and the product was obtained. The product was dissolved with deionized water, and 2 g sodium azide was added. The reaction was carried out at 85 °C for 24 h, and then, the solution was cooled to room temperature and 250 ml dichloromethane was added. The PEG was extracted into the organic phase and was separated, and the product was obtained by vacuum distillation. The product solution was deionized water, and argon was pumped to remove oxygen. Then, cysteamine hydrochloride and ammonium persulfate were added under the protection of argon. Reaction with 70 °C for 24 h. The pH value of the reaction solution was adjusted to alkaline by NaOH, and the product was extracted by dichloromethane and by reduced pressure distillation to obtain NH₂-PEG-N₃. NH₂-PEG-N₃ was dissolved in anhydrous DMSO, followed by EDC, NHS, and folic acid. After folic acid was completely dissolved, it was kept away from light for 24 h at room temperature. The mixed solution was put into a dialysis bag and dialyzed with deionized water for 48 h. The dialysis fluid was collected and freeze-dried to obtain the yellow powder product FA-PEG-N₃. Dissolve tocopherol succinate in anhydrous dichloromethane, and then add EDC, NHS, and propargyl carbamate ethyl dimercapto ethylamine after fully dissolving. The organic solvent was removed by vacuum distillation at room temperature for 24 h under light protection, and the product was dissolved with DMSO and placed into a dialysis bag for dialysis purification. After 24 h of dialysis, the dialysate was collected and freeze-dried to obtain the product Alkyne-SS-TPGS. FA-PEG-N₃ and Alkyne-SS-TPGS were added to a 50 ml round-bottom burner, dissolved in DMSO, and permeated with argon. After 10 min, cupric sulfate pentahydrate and sodium ascorbate were added and then permeated with argon for 10 min. The flask was sealed with a rubber plug, and the reaction was performed at 50 °C for 24 h. After the reaction, the solution was put into a dialysis bag and dialyzed with deionized water for 48 h. The dialysate was collected and freeze-dried to obtain FA-SS-TPGS as a product. The production of SPIO in this study is based on the established method previously developed [29].

2.3. In vivo studies

2.3.1. Infrared spectrogram

The infrared spectrogram of the sample was measured by a Nicolet Nexus 670 infrared spectrometer at room temperature. The sample was mixed with KBr and pressed with a scanning range of 500 cm⁻¹~4000 cm⁻¹.

2.3.2. Nuclear magnetic resonance hydrogen spectrum (¹H-NMR)

Hydrogen Nuclear Magnetic Resonance (¹H-NMR) was measured by the Mercury Plus 300 nuclear magnetic resonance apparatus (CDCl₃ as solvent and Si(CH₃)₄ as an internal standard) at room temperature.

2.3.3. Dynamic light scattering experiment

The dynamic light scattering experiment was carried out by a bi-200SM dynamic and static laser light scatterer produced by Brookhaven Corporation in the United States. The light source was an argon ion laser, the laser emission wavelength was 532 nm, the temperature was 25 °C, and the scattering light intensity was measured at 90 °C. The Contin and Cumulants were used to process the time correlation function. Before determination, the sample was filtered and dedusted with a 0.45 μm filter head.

2.3.4. Transmission electron microscopy (TEM)

The aggregation morphology of the polymer was observed by JEM2010 transmission electron microscopy (TEM) at an accelerated voltage of 80 keV. A drop of micelle solution was added to the copper wire and dried at room temperature. The polymer was dyed with a 2% phosphotungstate solution and dried at room temperature for 10 min.

2.3.5. DOX release efficiency

Using a UV-2501PC UV-visible spectrophotometer (Shimadzu Company), by measuring the absorbance at 485 nm, the standard operating curve of the drug concentration was calculated.

2.3.6. Preparation of Amphiphilic block micelles

Dialysis is a common method for the preparation of amphiphilic block micelles. First, 10 mg FA-SS TPGS, FA-TPGs, and TPGS were dissolved in 2 ml DMSO, stirring for 1 h. Then, the polymer solution was placed in a dialysis bag with a molecular weight of 3500 and dialyzed with deionized water at 25 °C for 24 h. The final dialysate was filtered with a 0.45 μm needle filter and then tested for dynamic light scattering.

2.3.7. In vitro MR imaging and cellular internalization of nanoparticles studies

The effect of the contrast agent is closely related to the relaxation rate of T2-weighted images. Relaxation rates of different probes will be measured to test the contrast effect of the probes on MR development. We matched the probes with six different concentrations, namely, 0, 0.03125, 0.0625, 0.1250, 0.2500, and 0.5000 mM, and then put the probes with six concentrations into six holes and put them into MR to measure the relaxation time of T2.

2.4. Preparation of DOX-Loaded nanoparticles

In situ loading of DOX/SPIO was achieved by the dialysis method. Then, 1 mg DOX, 1 mg SPIO, and 10 mg polymer were dissolved in 2 ml DMSO, and then the dialysis was performed in phosphate buffer solution (PBS) with a pH of 7.4 after full stirring for 2 h. The outer solution of the dialysis bag is changed every 3 h, and the unwrapped drugs will be removed by dialysis within 12 h. The determination method of drug content in micelles was as follows: micelles were destroyed by adding drug-carrying micelle solution into DMSO/PBS (v/v = 90:10) mixed solvent, the absorbance of the obtained system was measured at 372 nm after filtration, and the quantitative calculation was performed according to the standard curve. Then, 3 ml drug-loading micelles were loaded into a dialysis bag with a retained molecular weight of 3500 D, and 27 ml PBS dialysate with a pH of 7.4 was placed outside, which was released by shock at 37°C. At a specific time interval, 3 ml (V_e) was sampled from the external fluid of the dialysis bag, followed by 3 ml PBS to maintain the total volume unchanged. The concentration of DOX was determined by a standard working curve, and the determination was repeated three times for each sample. The cumulative release percentage (E_r) of drugs was calculated by the following formula (1):

$$E_r(\%) = \frac{V_e \sum_{i=1}^{n-1} C_i + V_0 C_n}{m_{\text{DOX}}} \times 100\% \quad (1)$$

m_{DOX} represents the mass of DOX in micelles, V_0 is the total volume of release medium ($V_0 = 30$ ml), C_i is the concentration of the i -th sample of DOX. DOX drug loading content (DLC %) was calculated according to Formula 2:

$$\text{DLC}(\%) = \frac{w_1}{w_2} \times 100\% \quad (2)$$

where w_1 is weight of loaded drug and w_2 is weight of the drug loaded polymer. DLC % of micelles was calculated by the absorbance value measured at 485 nm by an ultraviolet spectrophotometer.

The loading of SPIO nanoparticles in polymer micelles was determined by atomic absorption spectrophotometer (AAS). The micelles loaded with DOX/SPIO were added into a 1 M hydrochloric acid solution to completely dissolve the SPIO nanoparticles. Iron concentration was measured at a specific iron absorption wavelength (248.3 nm) according to a pre-established calibration curve. The SPIO loading content (SLC) was calculated from the following equation:

$$\text{SLC}(\%) = \frac{w_3}{w_2} \times 100\% \quad (3)$$

Where w_3 is weight of the loaded SPIO and w_2 is weight of polymer.

2.5. In vitro cytotoxicity

CCK-8 (Cell Counting Kit-8) Kit was used for biocompatibility and cytotoxicity experiments. The HepG2-ADM cells with good growth were inoculated into 96-well plates, with 4×10^3 cells per well, and then divided into different concentrations of 0, 50, 100, 150, 200, and 250 μg ml⁻¹ according to each blank probe, and four multiple wells were set for each concentration. Cells were cultured for 24 h and then CCK-8 was added for 24 h. Finally, the absorbance (OD) is measured at 450 nm using a microplate reader. According to the formula: growth inhibition rate = [(control group OD value – experimental group OD value)/control group OD value] × 100% to calculate the required cell survival rate.

In the cytotoxicity test of CCK-8, HepG2-ADM cells were inoculated into 96-well plates with 4×10^3 cells per well for 12 h. Then, the TPGS@DOX/SPIO, FA-TPGS@DOX/SPIO, FA-SS-TPGS@DOX SPIO, and Free DOX were divided into different concentrations of 10, 20, 30, 40, 50, and 60 μg/ml. Four multiple wells were set for each concentration. It was then left in an incubator for 24 h. Furthermore, 10 μl CCK-8 reagent was added to each well, and then placed in an incubator for 2–4 h. Then, the absorbance (OD) was measured at 450 nm using a

microplate reader. After that, the growth inhibition rate was calculated using the formula: [(CONTROL group OD value – experimental group OD value)/control group OD value] × 100% .

2.6. *In vitro* uptake assay

Flow cytometry was used to quantitatively analyze the fluorescence intensity of DOX in HepG2-ADM cells. Drug-resistant liver cancer cells were inoculated into 6-well plates and cultured in a constant temperature incubator for 24 h. After removing and discarding the medium, TPGS@DOX/SPIO, FA-TPGS@DOX/SPIO, FA-SS-TPGS@DOX/SPIO, and Free DOX. The dosage was 200 μl /well, and the concentration was 10 $\mu\text{g ml}^{-1}$. Then, trypsin was added to each well for 3 min for digestion. Then, the digested solution was collected for centrifugation, the supernatant was removed, and 1 ml PBS was added to re-suspend the cells. Finally, flow cytometry was performed, and the excitation wavelength was 488 nm. The emission wavelength is 575 nm.

Prussian blue staining was performed to detect the cellular uptake of SPIO. HepG2-ADM cells were first inoculated into 24-well plates, and the cell density was set at 2×10^5 cells/well. Then, HepG2-ADM cells were cultured in a constant temperature incubator for 24 h, and the medium was discarded. Then, 10 $\mu\text{g ml}^{-1}$ of each TPGS/SPIO, FA-TPGS/SPIO, and FA-SS-TPGS/SPIO were added to three different blank probes prepared by us, and three multiple holes in each group were set as reference. After incubation for 24 h, the culture medium was discarded and rinsed three times with PBS. Then it was fixed with 4% paraformaldehyde for 10–20 min and washed with distilled water for 2–3 min. Add Prussian blue dye and stain for 4–8 h. After rinsing, add the nucleus-solid red dye and rinse for 3 min. Then, the 24-well plate was sucked clean and dried, and the Prussian blue particles were observed under a microscope to enter HepG2-ADM cells.

DAPI staining was performed to confirm the uptake of nano-polymers by cells. In this study, drug-resistant liver cancer cells were inoculated into a confocal petri dish with 1×10^6 cells/well. After 24 h, TPGS@DOX/SPIO, FA-TPGS@DOX/SPIO, FA-SS-TPGS@DOX/SPIO, and Free DOX. The concentrations were 10 $\mu\text{g ml}^{-1}$ and 30 $\mu\text{g ml}^{-1}$. After 24 h, the medium was discarded and 1 ml DAPI dye was added. Finally, the laser confocal microscope was used to observe. The excitation wavelength of DOX and DAPI was 485 nm and 358 nm, respectively. DOX and DAPI have emission wavelengths of 590 nm and 455 nm, respectively.

2.7. *In vitro* apoptosis analysis

HepG2-ADM cells were inoculated into confocal petri dishes at a density of 1×10^6 /well. After 24 h, the medium was discarded and TPGS@DOX/SPIO, FA-TPGS@DOX/SPIO, FA-SS-TPGS@DOX SPIO, and Free DOX were added at concentrations of 10 $\mu\text{g/ml}$ and 30 $\mu\text{g ml}^{-1}$. Furthermore, 24 h later, the discarded medium was removed, and then, 50 μl of calcein-AM/PI was added to each confocal petri dish, and they were observed under a confocal microscope after 15 min.

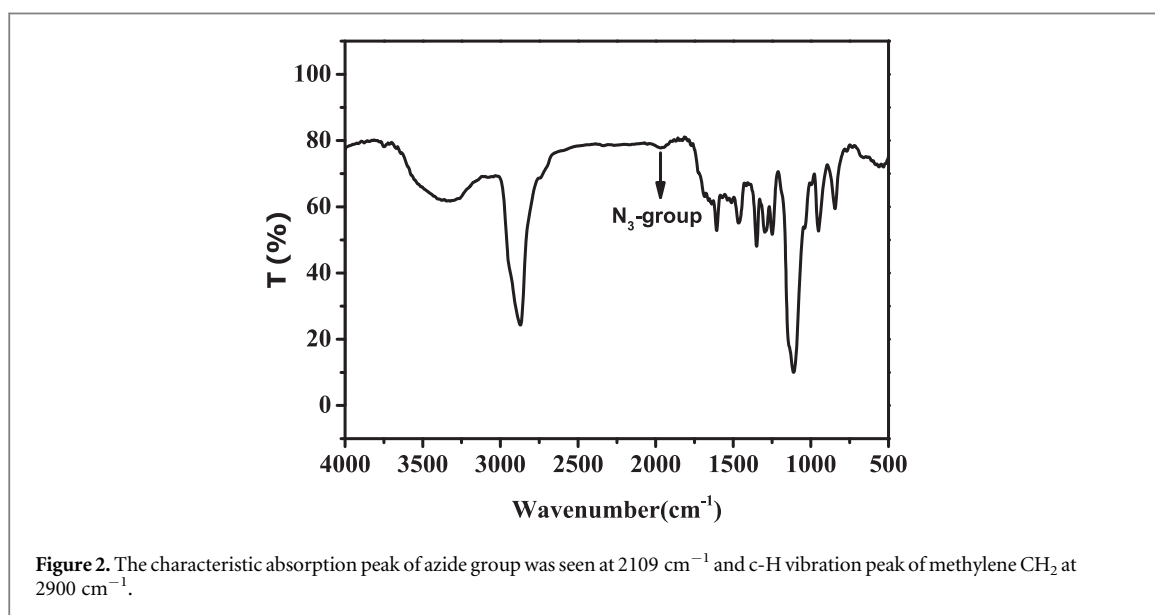
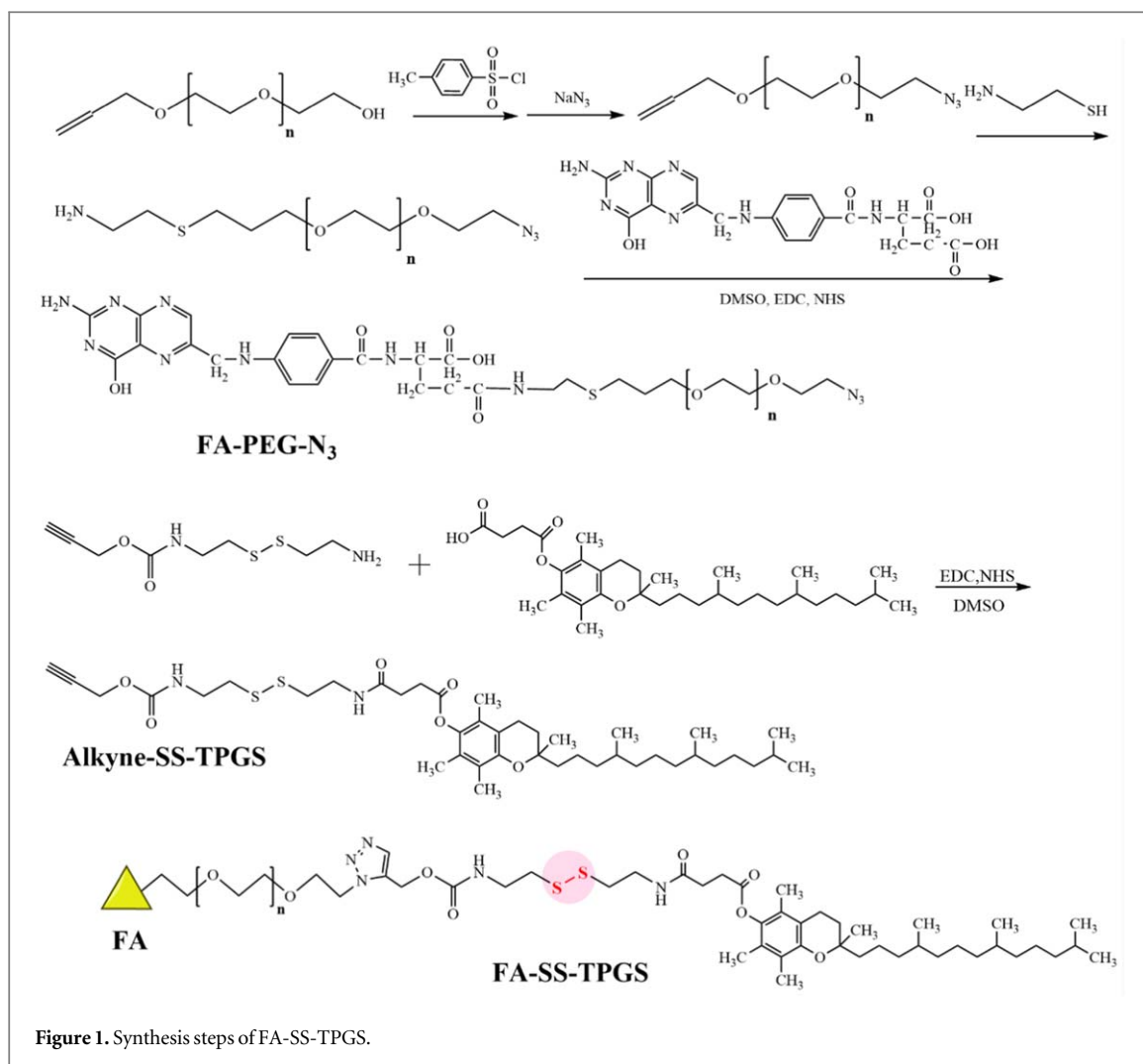
3. Result and discussion

3.1. Characterization of synthesized copolymer

TPGS nanoparticles were prepared by a series of reactions. The overall design is shown in figure 1. Figure 2 shows the infrared spectrum of N3-PEG-FA. The characteristic absorption peak of the azide group was seen at 2109 cm^{-1} and c-H vibration peak of methylene CH_2 at 2900 cm^{-1} . According to the nuclear magnetic resonance hydrogen spectrum (1 H-NMR) of N3-PEG-FA in figure 3, it was observed that the proton on the benzene ring of folic acid was in the range of 6.5–8 ppm, and the methylene H was in the range of 3.5 ppm. IR spectrum of alkyne-SS-VES showed that the C-H vibrational peak was located at 2900 cm^{-1} , and the C=O stretching vibrational absorption peak was located at 1750 cm^{-1} . As figure 4 showed, the C-H vibrational peak is located at 2900 cm^{-1} , and the C=O stretching vibrational absorption peak is located at 1750 cm^{-1} . The characteristic peaks at 3.5 and 4.25 PPM, showed in figure 5, belong to methylene on propargyl carbamate ethyl dimercaptoethylamine. Thus, alkyne-SS-VES was successfully prepared. The H NMR of Final product FA-SS-TPGS was shown in figure 6.

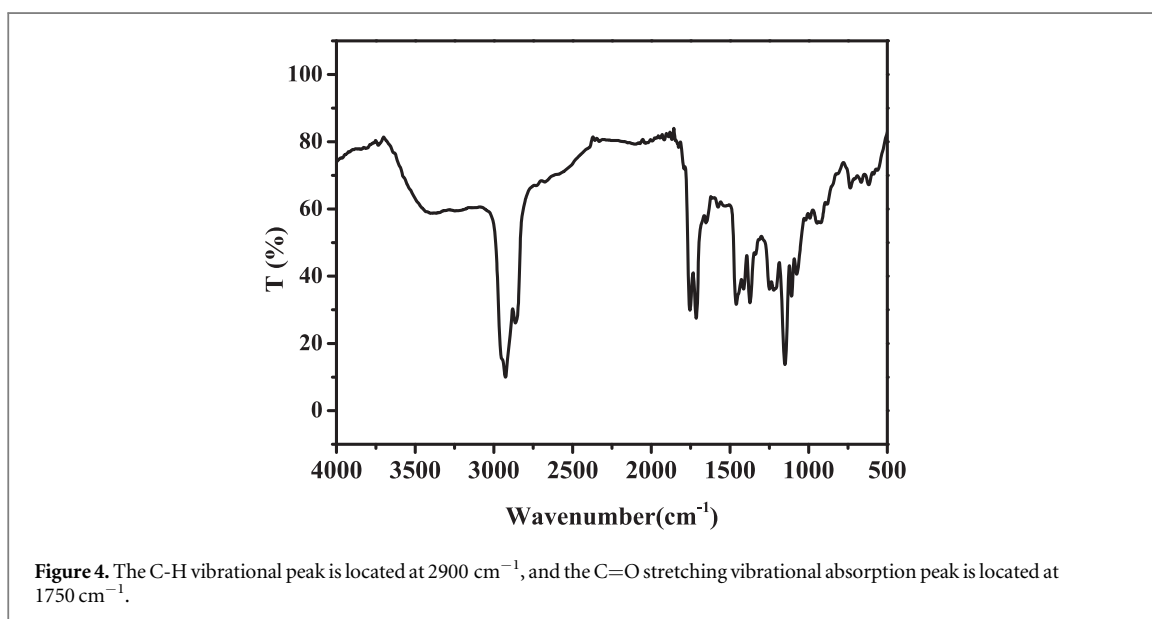
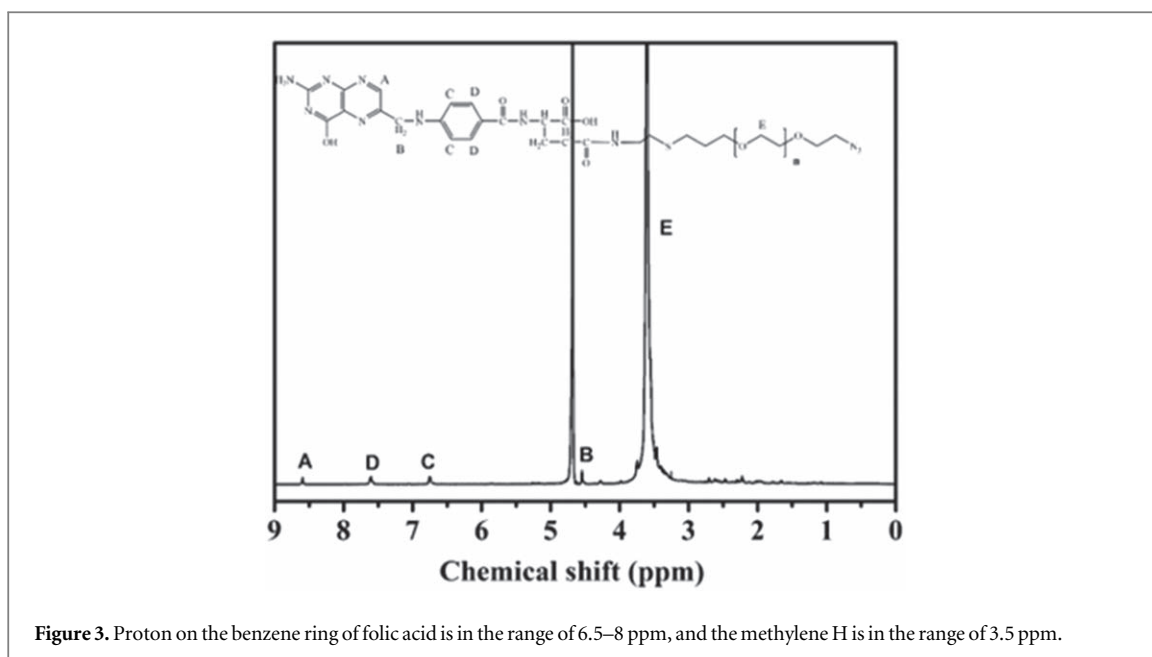
Figure 7 shows the particle size distribution and morphology test results of blank FA-SS-TPGS micelles and FA-SS-TPGS@DOX/SPIO micelles. According to the DLS test results, the average particle size of blank FA-SS-TPGS micelles was about 95.6 nm, and the average particle size of FA-SS-TPGS@DOX/SPIO micelles was about 134.6 nm. The significant increase in particle size was mainly caused by the entry of hydrophobic DOX and SPIO into the hydrophobic core of nanoparticles. TEM observation showed that FA-SS-TPGS self-assembled spherical nanoparticles in aqueous solution.

It was also found that the mean particle size of micelles observed by TEM was smaller than that by DLS, probably because DLS tests were carried out in aqueous solution, while TEM observations were carried out in a dry environment. In addition, TEM results also indicated that FA-SS-TPGS@DOX/SPIO nanoparticles also



form spherical nanoparticles. It could also be seen that the particle size of FA-SS-TPGS@DOX/SPIO was larger than that of FA-SS-TPGS nanoparticles.

As can be seen from table 1, the prepared FA-SS-TPGS had high loading capacity for both DOX and SPIO. Compared with TPGS, FA-SS-TPGS had a better loading capacity for DOX and SPIO.

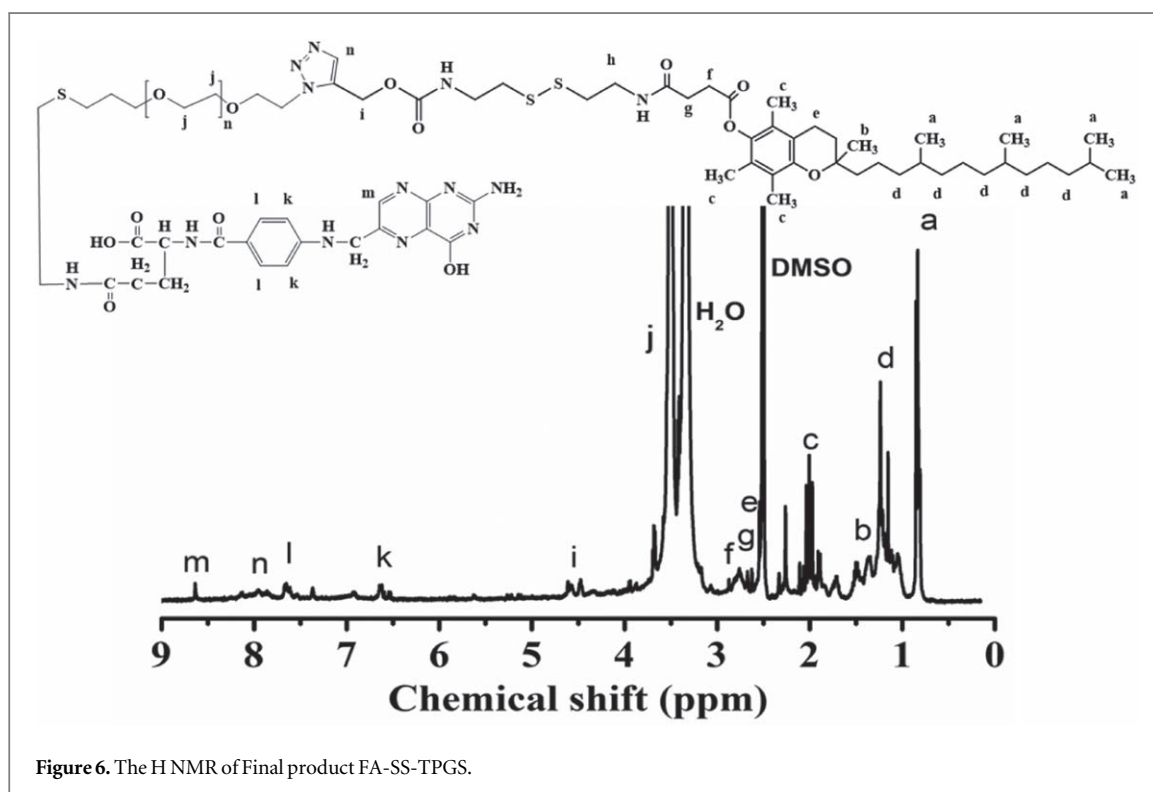
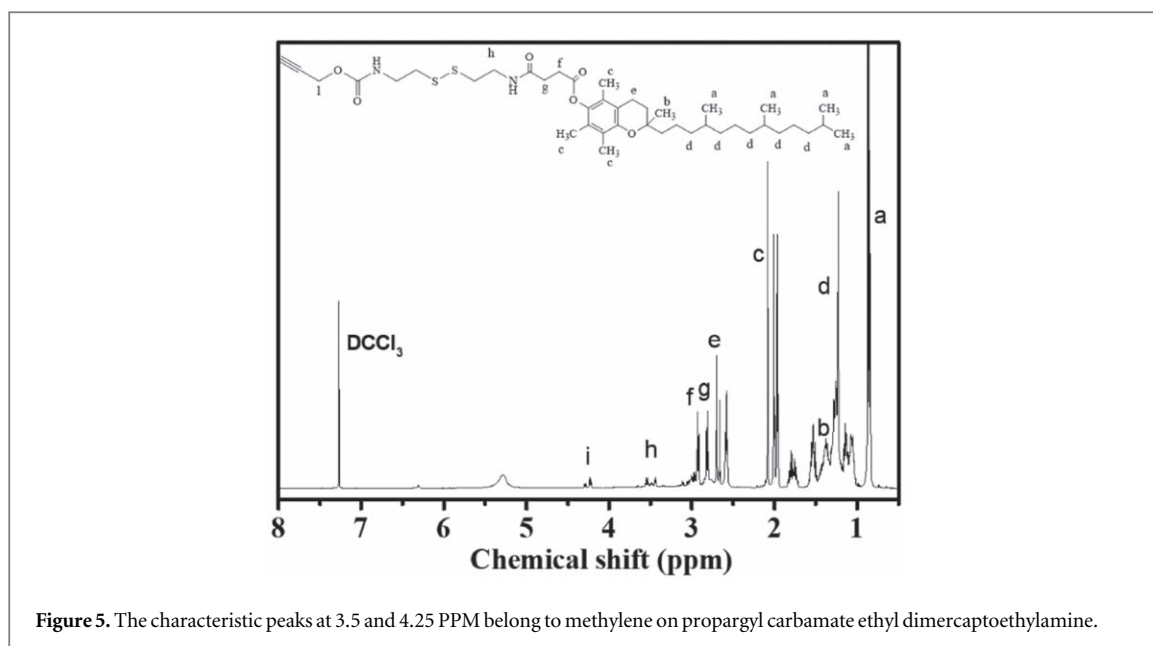


3.2. Drug release rate testing

The *in vitro* release experiments for DOX were conducted under two conditions: in the presence and absence of glutathione (GSH) in phosphate-buffered saline (PBS) at a pH of 7.4. The results are presented in figure 8. We released the drug at a single concentration and acknowledged that if different concentrations of GSH were utilized, varying release rates would occur. The drug release data demonstrated that the FA-SS-TPGS micelles exhibited a reductant-triggered release profile, as evidenced by 100% release of DOX from the micelles within 12 h in the presence of GSH. In contrast, only approximately 40% release of DOX was observed under non-reductive conditions within 24 h. The accelerated DOX release under reductive conditions was attributed to the degradation of the disulfide linkages in the micelles. The FA-SS-TPGS micelles could be effectively mitigated, leading to a significant enhancement in therapeutic efficacy and successful overcoming of MDR.

3.3. MRI contrast measurement

Figure 9 showed the magnetic properties of nanoparticles loaded with SPIO. SPIO based nanoparticles could shorten the T2 relaxation time. TPGS@SPIO containing SPIO had a magnetic conductivity of about $126.8\text{ Fe mM}^{-1}\text{ s}^{-1}$. The magnetic properties of FA-TPGS@SPIO containing SPIO was about $261.3\text{ Fe mM}^{-1}\text{ s}^{-1}$. FA-SS-TPGS@SPIO containing SPIO had a magnetic conductivity of approximately $230\text{ Fe mM}^{-1}\text{ s}^{-1}$. It can be



seen that FA-TPGS and FA-SS-TPGS, two novel TPGS derivatives prepared in this study, had better magnetic properties than TPGS when they were loaded SPIO. It verified that the NPs were useful for MRI imaging.

3.4. *In vitro* cellular uptake studies

As shown in figure 10, the experiments evaluated the effects of FA and disulfide bonds on the cellular uptake behavior and intracellular distribution of DOX in HepG2-ADM cells. Compare with DOX-loaded NPs, free DOX was hardly located in the HepG2-ADM cells, which because of the reduced susceptibility of the cells. TPGS@DOX/SPIO was mainly accumulated throughout the cytoplasm of HepG2-ADM cells and substantially less accumulated in the nuclei. Meanwhile, TPGS could strengthen drug accumulation in drug resistant cells, which may be attributed to the TPGS property as an inhibitor of P-gp [30]. FA-SS-TPGS@DOX/SPIO and FA-TPGS@DOX/SPIO nanoparticles presented strong DOX fluorescence accumulated in the cytosol, and weak

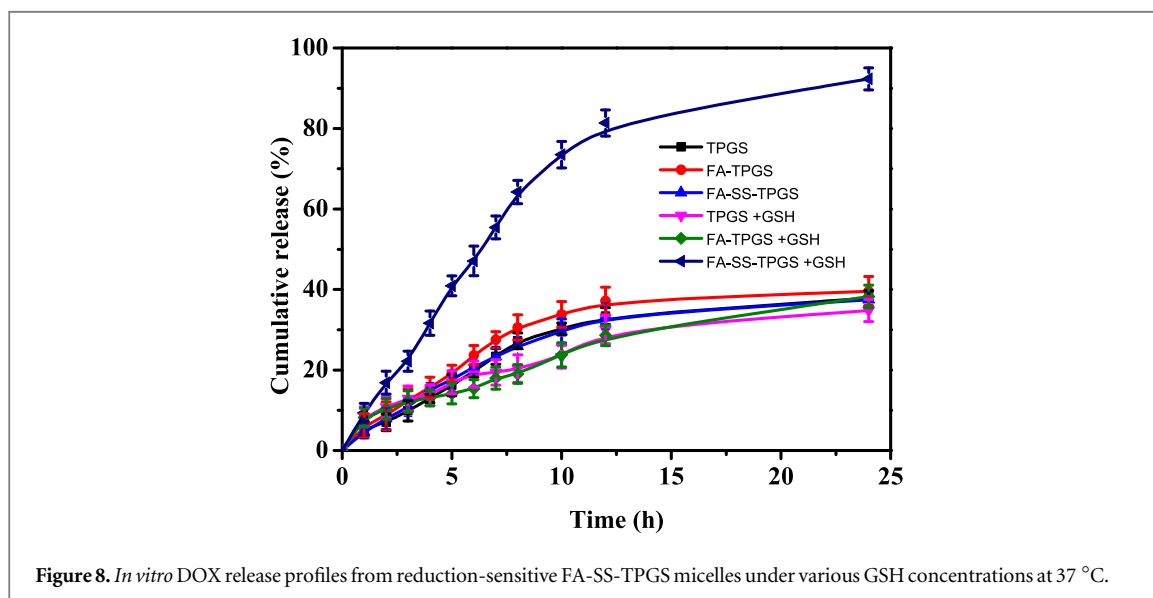
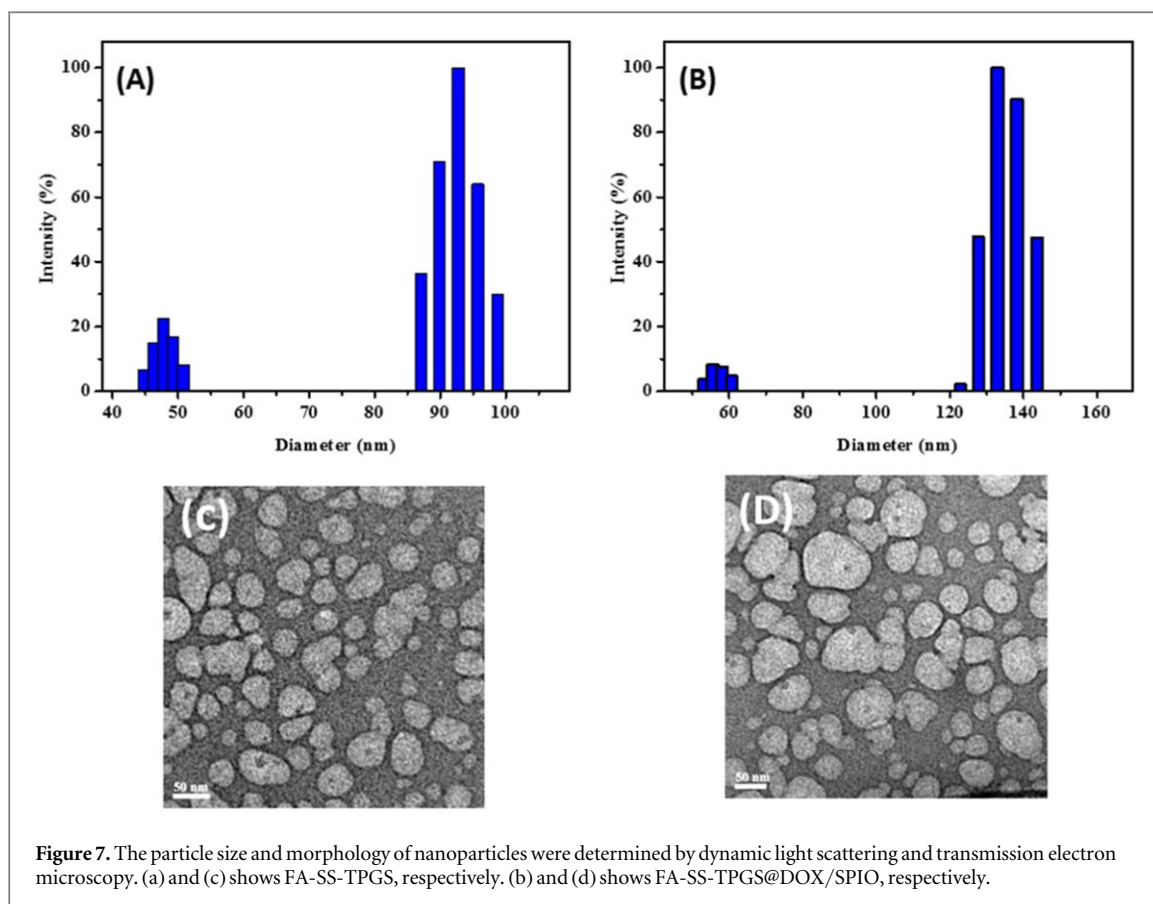
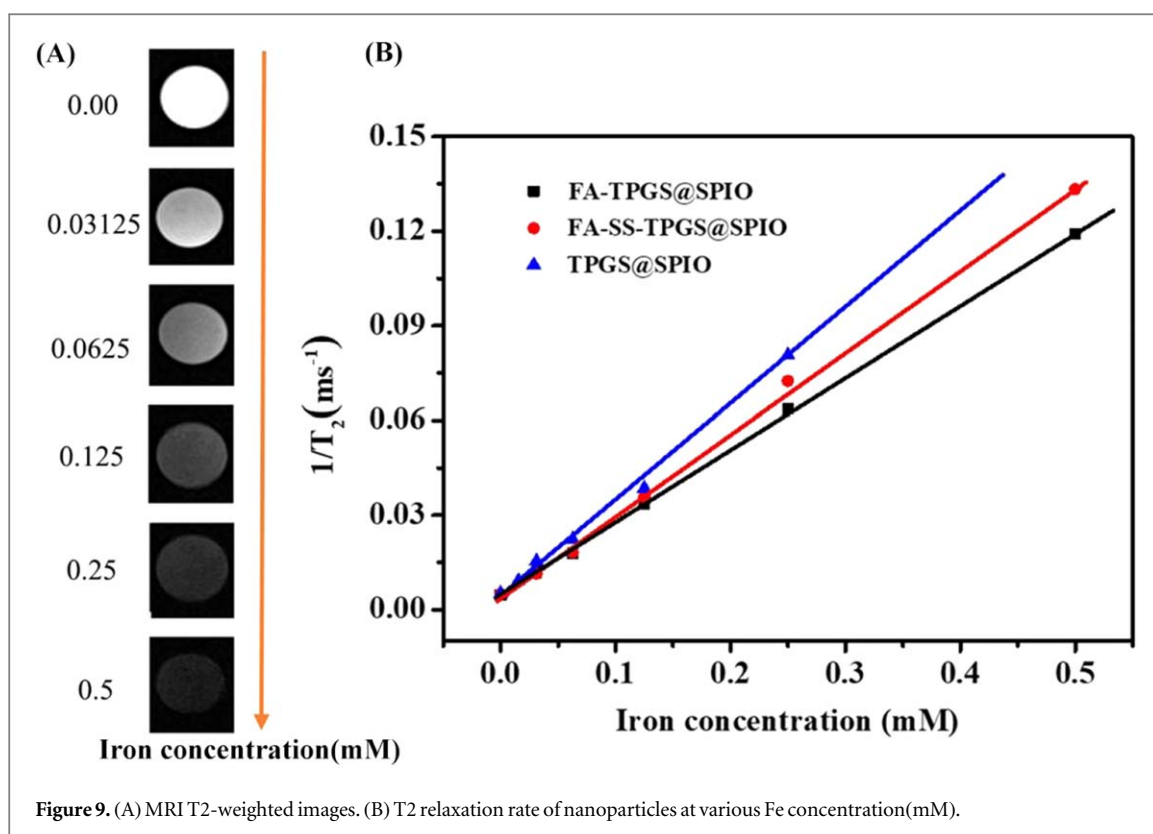


Table 1. Characteristics of blank micelles and DOX/SPIO micelles.

Sample code	Blank micelles		DOX/SPIO-loaded micelles			
	Diameter (nm)	PDI	Diameter (nm)	PDI	DLC (%)	SLE (%)
FA-SS-TPGS	95.6 ± 2.7	0.06 ± 0.01	134.6 ± 1.7	0.10 ± 0.01	6.6	7.5
FA-TPGS	88.7 ± 2.0	0.09 ± 0.02	127.3 ± 3.6	0.12 ± 0.04	6.2	6.9
TPGS	93.5 ± 1.7	0.15 ± 0.02	125.8 ± 2.3	0.10 ± 0.04	5.3	7.3



fluorescence accumulated in the nuclei. FA-SS-TPGS@DOX/SPIO showed significant red fluorescence throughout the cytoplasm, which manifested enhanced cell uptake. The results provided visual evidence supporting the involvement of folate receptor-mediated endocytosis in the uptake and intracellular distribution of DOX in these cells. The obtained results are consistent with the mechanism of folate receptor-mediated endocytosis [31].

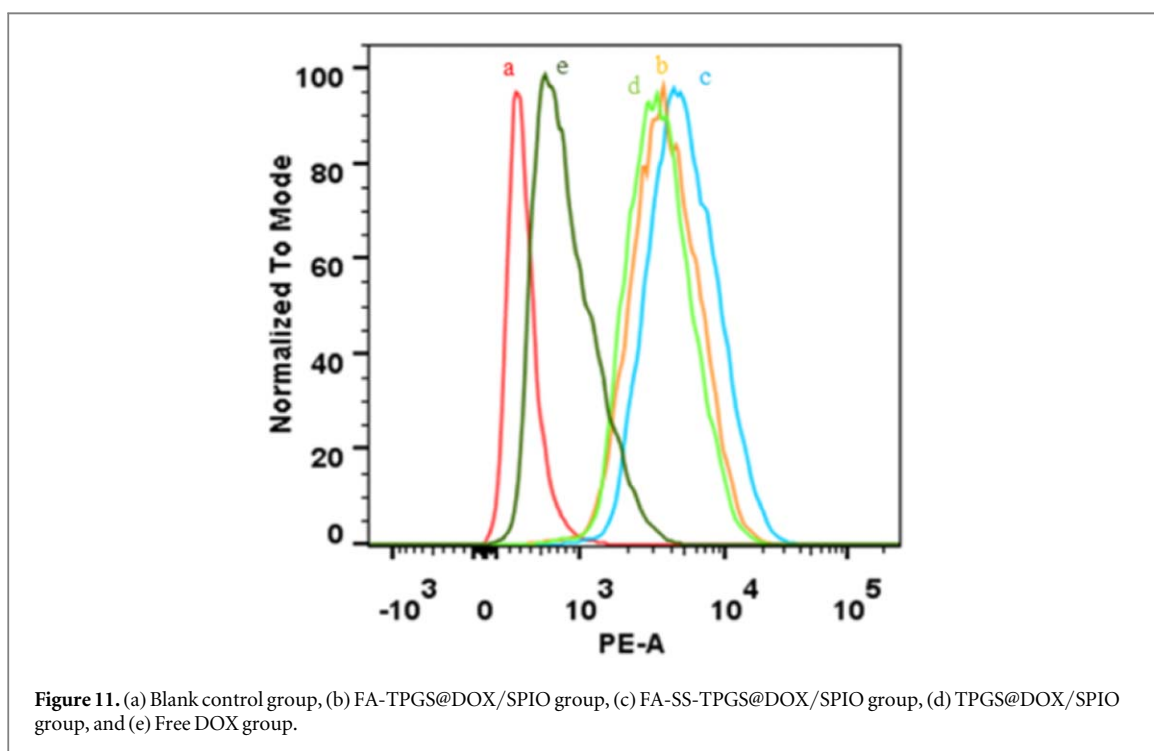
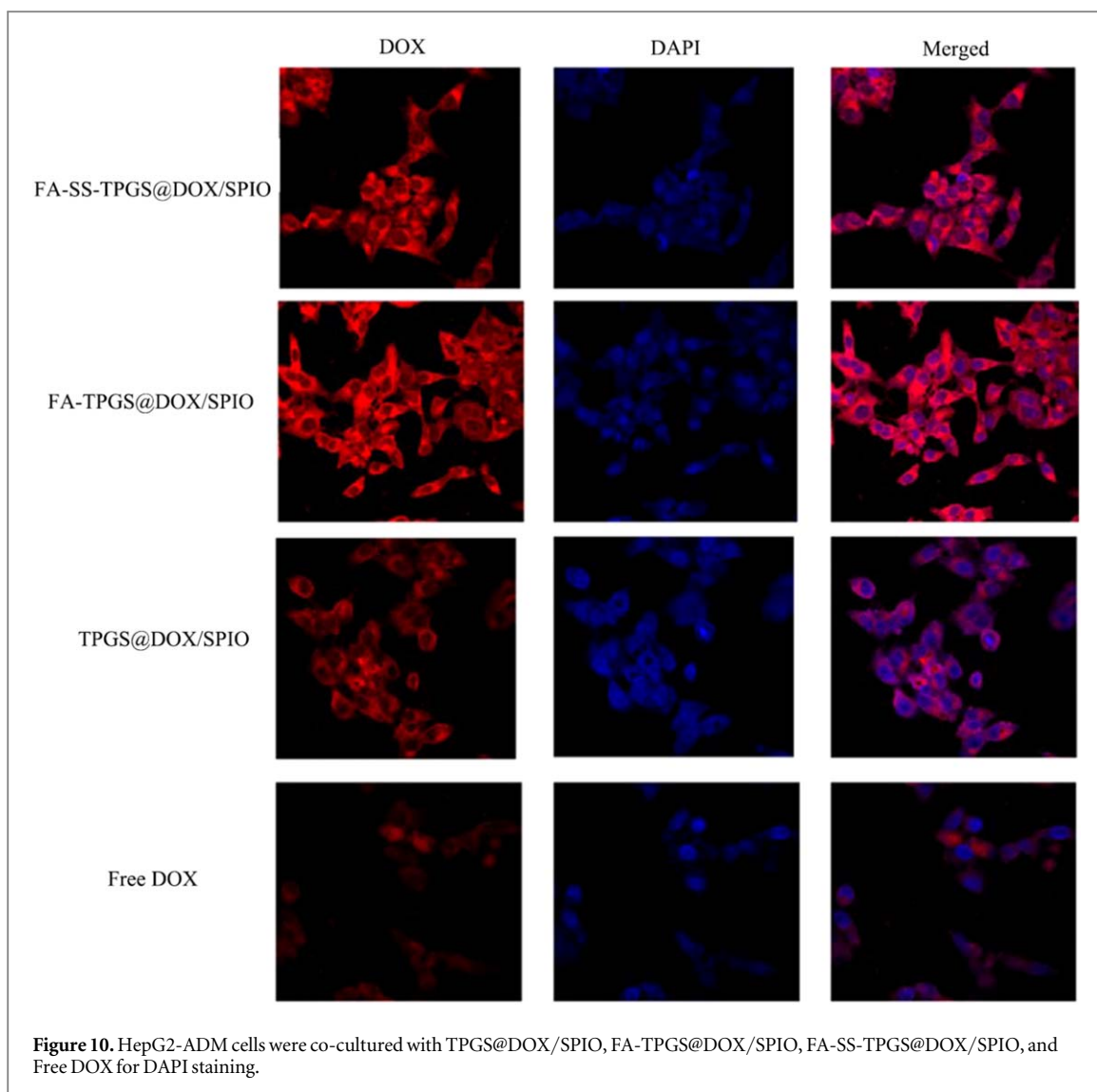
In order to verify the HepG2-ADM cells uptake rate induced by the DOX-loaded NPs, flow cytometry was performed to carry out a quantitative analysis of the fluorescence intensity. In the experiment, 10 $\mu\text{g/ml}$ TPGS@DOX/SPIO, FA-TPGS@DOX/SPIO, FA-SS-TPGS@DOX/SPIO, and Free DOX were used to incubate HepG2-ADM cells for 4 h. According to figure 11, flow cytometric analysis revealed that HepG2-ADM cells treated with nanoparticles that were decorated with an FA-targeting ligand or contained disulfide bond linkages exhibited significantly higher fluorescence intensity of DOX compared to nanoparticles that lacked FA and disulfide bonds. Moreover, the fluorescence intensity in the cells showed that fluorescence intensity of FA-SS-TPGS@DOX/SPIO group was the highest among the four drugs. This was consistent with the results of the first experiment. This results proved the ability of DOX-loaded NPs could overcome MDR in HepG2-ADM cells. Especially, FA-SS-TPGS@DOX/SPIO can enhance anticancer effects to a greater degree with a collaborative so that it could effectively overcome MDR in cancer chemotherapy.

The *in vitro* cellular uptake effects of the star polymeric nanoparticles were demonstrated using Prussian blue staining. According to figure 12, unloaded medicine TPGS/SPIO, FA-TPGS/SPIO, and FA-SS-TPGS/SPIO could be seen in HepG2-ADM cells. It could be found remarkable blue fluorescence in the FA-SS-TPGS/SPIO group. These findings are consistent with results reported in the literature [22]. Based on the experiments, FA-SS-TPGS@DOX/SPIO could be used as anticancer drugs against HepG2-ADM cells.

3.5. *In vitro* cytotoxicity

The cytotoxicity of blank NPs was first tested by using HepG2-ADM cells treated with different NP concentrations (0, 50, 100, 150, 200, and 250 $\mu\text{g ml}^{-1}$). As figure 13 showed that when the concentration of each blank vector reached 300 $\mu\text{g ml}^{-1}$, the survival rate of cells could still exceed 70%. It suggested that the blank NPs at the tested concentrations exhibited nontoxicity on HepG2-ADM.

So as to assess the cytotoxicity of DOX-loaded NPs to drug resistant cells, DOX-loaded NPs were tested by using HepG2-ADM cells treated with different NP concentrations (10, 20, 30, 40, 50, and 60 $\mu\text{g ml}^{-1}$). According to figure 14, DOX-loaded NPs enhanced cell cytotoxicity on HepG2-ADM cells. Free DOX exhibited significantly lower cell cytotoxicity compared with that of DOX-loaded NPs. The HepG2-ADM cells exhibited obvious drug resistance to Free-Dox with the drug incubation concentration of 10–60 $\mu\text{g ml}^{-1}$. Meanwhile,



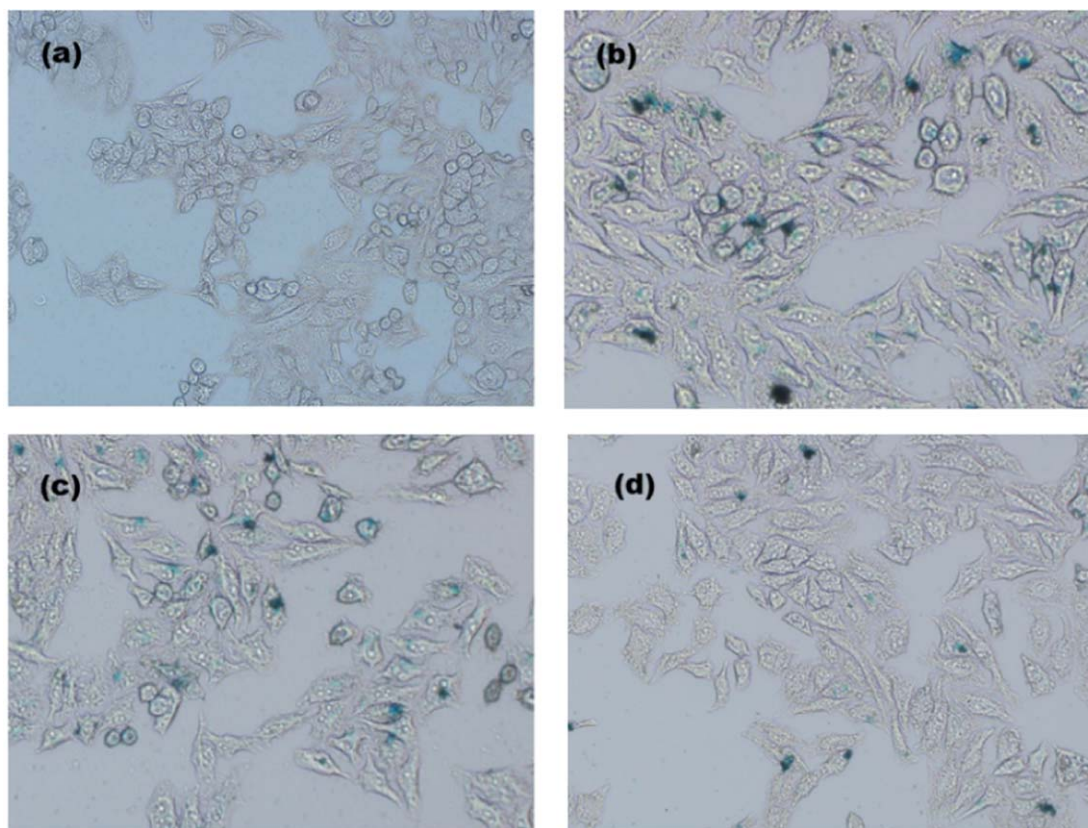


Figure 12. Prussian blue staining of HepG2-ADM cells (scale 100 μm). (a) Normal growth of HepG2-ADM cells, (b) FA-SS-TPGS/SPIO group, (c) FA-TPGS/SPIO group, and (d) TPGS/SPIO group.

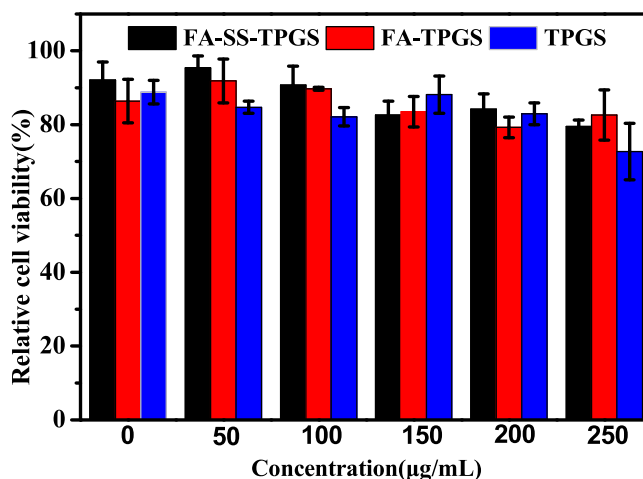


Figure 13. The survival rate of HepG2-ADM cells of blank materials at different concentrations.

DOX-loaded NPs could overcome the drug resistance of HepG2-ADM cells, so that they could increase the cell cytotoxicity. With the drug concentration grew, the cell cytotoxicity of Dox- loaded NPs appeared significant increased. Furthermore, the cytotoxicity of FA-SS-TPGS@DOX/SPIO was the most significant among the three NPs. In summary, DOX-loaded NPs maintain the pharmacological activity of DOX. FA-SS-TPGS@DOX/SPIO overcame MDR of HepG2-ADM cells effectively.

3.6. Cell apoptosis analysis

HepG2-ADM cells treated with Free DOX and DOX-loaded NPs. Then they observed by fluorescence microscopy. As figure 15 shown, we could obviously found distinction of the cells treated by free-DOX and

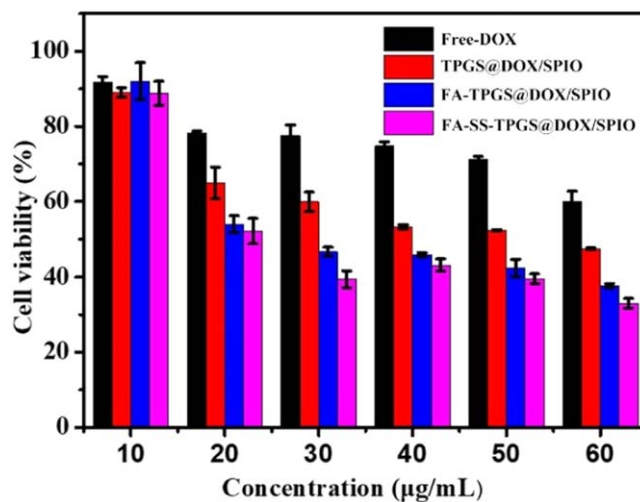


Figure 14. The survival rate of HepG2-ADM cells in different concentrations of drugs.

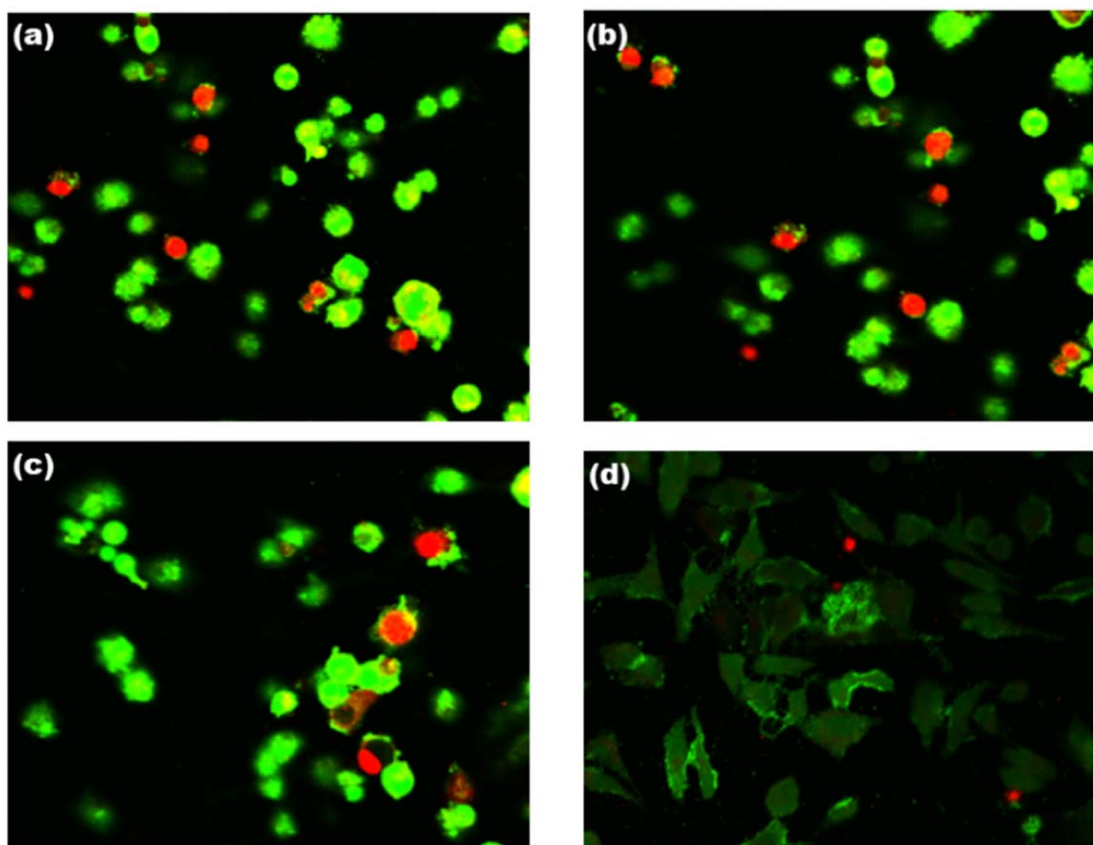


Figure 15. HepG2-ADM cells by calcein-AM/PI double staining (scale: 100 μm) (a) FA-SS-TPGS@DOX/SPIO group, (b) FA-TPGS@DOX/SPIO group, (c) TPGS@DOX/SPIO group, and (d) Free DOX group.

DOX-loaded NPs at the concentration of 30 $\mu\text{g ml}^{-1}$. Among the four groups of drugs, the cells in the Free DOX maintained well cellular morphology. In comparison, the DOX-loaded NPs could significantly influence cellular morphology. Some nuclei shrank as well as apoptosis bodies appeared, which was the most obvious after treatment with FA-SS-TPGS@DOX/SPIO. The above results showed that FA-SS-TPGS@DOX/SPIO exhibited the strongest antitumor efficacy.

4. Conclusions

In this study, we successfully synthesized folic acid and disulfide bond modified FA-SS-TPGS@DOX/SPIO. The chemical characteristics of the polymer were confirmed through various tests such as infra-red spectrogram, dynamic light scattering experiment, and ¹H NMR. Due to these characteristics, the amphiphilic nature of the polymer enabled it to self-assemble into spherical nanoparticles with an average size of approximately 95.6 nm. The amphiphilic nature of the polymer allowed it to self-assemble into spherical nanoparticles with an average size of approximately 95.6 nm. These nanoparticles served as theranostic agents after loading with DOX and SPIO. Drug release experiments demonstrated that the nanoparticles rapidly released DOX in a high GSH environment, which is often found in cancer cells. Among the tested nanoparticles, FA-SS-TPGS@DOX/SPIO was found to be the most effective. *In vitro* cellular uptake and cytotoxicity assays indicated that FA-SS-TPGS@DOX/SPIO exhibited high intracellular uptake. Additionally, the nanoparticles showed a significant change in the T2 signal, indicating their potential for imaging purposes. In conclusion, FA-SS-TPGS@DOX/SPIO nanoparticles demonstrated great potential as theranostic agents for drug-resistant tumors. Their ability to target tumor cells, release drugs in response to the intracellular environment, and provide imaging capabilities make them promising candidates for overcoming multidrug resistance and improving cancer treatment outcomes.

Acknowledgments

This study was funded by the Guangzhou Health Science and Technology project (grant number 20221A010014, 20241A011022). The National Natural Science Foundation of China (82271938). The Guangdong Basic and Applied Basic Research Foundation (2023A1515012320), the Science and Technology Project of Guangzhou (2023A03J0969).

Data availability statement

All data that support the findings of this study are included within the article (and any supplementary files).

Author contribution

This passage describes the roles and contributions of various authors in a particular study. ZL designed and performed the study, while HY was responsible for drug preparation. FX conducted the cell culture portion of the study. XJ, XZ, and HH all played a role in conceiving and designing the study, performing it, authoring or reviewing drafts of the paper, and approving the final version. Overall, all authors contributed to the article and approved its final submission.

Ethics statement

This study was approved by the Ethics Committee of Guangzhou Red Cross Hospital of Jinan University.

Conflict of interest

The authors report no conflict of interest in the present study.

ORCID iDs

Zhuoran Li  <https://orcid.org/0000-0002-5236-1575>

Haowei Huang  <https://orcid.org/0000-0002-8029-1981>

References

- [1] Hill B T, Whelan R D H, Hurst H C and Mcclean S 2015 Identification of a distinctive P-glycoprotein-mediated resistance phenotype in human ovarian carcinoma cells after their *in vitro* exposure to fractionated X-irradiation *Cancer*. **73** 2990–9
- [2] Boumahdi S and de Sauvage F J 2019 The great escape: tumour cell plasticity in resistance to targeted therapy *Nat. Rev. Drug Discovery* **19** 39–56

- [3] Fu Q *et al* 2020 Organ index of immunological and anti-tumor effect of intratumor injection of penicillin sodium combined with chemotherapy drug for tumor-bearing mice *Journal of Clinical Oncology* **38** e16134
- [4] Lashof-Sullivan M, Kim M P, Tzeng C and Indolfi L 2020 Novel targeted and sustained drug delivery therapy for localized pancreatic cancer: Validation in porcine models and minimally invasive surgical feasibility in human cadavers *Journal of Clinical Oncology* **38** e16747
- [5] Torchilin V P 2001 Structure and design of polymeric surfactant-based drug delivery systems *J. Controlled Release* **73** 137–72
- [6] Maeda H, Bharate G Y and Daruwalla J 2009 Polymeric drugs for efficient tumor-targeted drug delivery based on EPR-effect *European Journal of Pharmaceutics and Biopharmaceutics* **71** 409–19
- [7] Sakai-Kato K *et al* 2015 General considerations regarding the in vitro and in vivo properties of block copolymer micelle products and their evaluation *J. Control. Release* **210** 76–83
- [8] Zhou L W H and Li Y 2018 Stimuli-responsive nanomedicines for overcoming cancer multidrug resistance *Theranostics* **8** 1059–74 (PMID: 29463999; PMCID: PMC5817110) (PMID: 29463999; PMCID: PMC517110)
- [9] Zhu Y X, Jia H R, Gao G, Pan G Y and Wu F G 2019 Mitochondria-acting nanomicelles for destruction of cancer cells via excessive mitophagy/autophagy-driven lethal energy depletion and phototherapy *Biomaterials* **232** 119668
- [10] Fan C H *et al* 2016 Ultrasound/Magnetic targeting with SPIO-DOX-microbubble complex for image-guided drug delivery in brain tumors *Theranostics* **6** 1542–56
- [11] Li D *et al* 2021 Ultrasound-enhanced fluorescence imaging and chemotherapy of multidrug-resistant tumors using multifunctional dendrimer/carbon dot nanohybrids *Bioact. Mater.* **6** 11
- [12] Collnot E M, Baldes C, Schaefer U F, Edgar K J, Wempe M F and Lehr C M 2010 Vitamin E TPGS P-glycoprotein inhibition mechanism: influence on conformational flexibility, intracellular ATP levels, and role of time and site of access *Mol. Pharmaceutics* **7** 642–51
- [13] Zhang Z, Tan S and Feng S S 2012 Vitamin E TPGS as a molecular biomaterial for drug delivery *Biomaterials* **33** 4889–906
- [14] Zhang Z and Feng S S 2006 The drug encapsulation efficiency, in vitro drug release, cellular uptake and cytotoxicity of paclitaxel-loaded poly(lactide)-tocopheryl polyethylene glycol succinate nanoparticles *Biomaterials* **27** 4025–33
- [15] Zhang Z, Lee S H, Gan C W and Feng S S 2008 *In vitro* and *in vivo* investigation on PLA-TPGS nanoparticles for controlled and sustained small molecule chemotherapy *Pharm. Res.* **25** 1925–35
- [16] Xiao Z, Su Z, Han S, Huang J and Shuai X 2020 Dual pH-sensitive nanodrug blocks PD-1 immune checkpoint and uses T cells to deliver NF- κ B inhibitor for antitumor immunotherapy *Sci. Adv.* **6** eaay7785
- [17] Dong S, Guo X, Han F, He Z and Wang Y 2022 Emerging role of natural products in cancer immunotherapy *Acta Pharm. Sin.* **B** (012-003)
- [18] Hao T, Chen D, Liu K, Qi Y and Li Z 2015 Micelles of d- α -tocopheryl polyethylene glycol 2000 succinate (TPGS 2K) for doxorubicin delivery with reversal of multidrug resistance *ACS Appl. Mater. Interfaces* **7** 18064–75
- [19] Góngora-Benítez M, Tulla-Puche J and Albericio F 2014 Multifaceted roles of disulfide bonds. Peptides as therapeutics *Chem. Rev.* **114** 901–26
- [20] Chen Y *et al* 2017 Enzymatic PEG–Poly(amine–co–disulfide ester) Nanoparticles as pH- and Redox-Responsive Drug Nanocarriers for Efficient Antitumor Treatment *ACS Appl. Mater. Inter.* **9** 30519–35
- [21] Kefayat A, Hosseini M, Ghahremani F, Jolfaie N A and Rafienia M 2022 Biodegradable and biocompatible subcutaneous implants consisted of pH-sensitive mebendazole-loaded/folic acid-targeted chitosan nanoparticles for murine triple-negative breast cancer treatment *Journal of Nanobiotechnology* **20** 169
- [22] Canal F, Vicent M J, Pasut G and Schiavon O 2010 Relevance of folic acid/polymer ratio in targeted PEG-epirubicin conjugates *J. Controlled Release* **146** 388–99
- [23] Yang H, Wang N and Yang R 2021 Folic Acid-Decorated β -Cyclodextrin-Based Poly(ϵ -caprolactone)-dextran Star Polymer with Disulfide Bond-Linker as Theranostic Nanoparticle for Tumor-Targeted MRI and Chemotherapy *Pharmaceutics* **14** 52
- [24] Guan Q, Guo R, Huang S, Zhang F and Cao Z 2020 Mesoporous polydopamine carrying sorafenib and SPIO nanoparticles for MRI-guided ferroptosis cancer therapy *J. Controlled Release* **320** 392–403
- [25] Shen Z *et al* 2017 Multifunctional theranostic nanoparticles based on exceedingly small magnetic iron oxide nanoparticles for T1-weighted magnetic resonance imaging and chemotherapy *ACS nano*. 10992
- [26] Hasan S, Kudithipudi V, Thai N V and Kirichenko A V 2016 Stereotactic Body Radiation Therapy (SBRT) With Functional Treatment Planning for Hepatocellular Carcinoma (HCC) in Patients With Early-Stage Cirrhosis *Int. J. Radiat. Oncol. Biol. Phys.* **96** E182
- [27] Karlsson H L, Cronholm P, Gustafsson J and Möller L 2008 Copper oxide nanoparticles are highly toxic: a comparison between metal oxide nanoparticles and carbon nanotubes *Chem. Res. Toxicol.* **21** 1726–32
- [28] Su H *et al* 2013 Amphiphilic starlike dextran wrapped superparamagnetic iron oxide nanoparticle clusters as effective magnetic resonance imaging probes *Biomaterials* **34** 1193–203
- [29] Huikang Y *et al* 2019 Enzymatic PEG–Poly(amine-co-disulfide ester) nanoparticles as pH- and redox-responsive drug nanocarriers for efficient antitumor treatment *ACS Appl. Mater. Inter.* **9** 30519–35
- [30] Guo Y, Chu M, Tan S, Zhao S and Zhang Z 2013 Chitosan-g-TPGS nanoparticles for anticancer drug delivery and overcoming multidrug resistance *Mol. Pharmaceutics* **11** 59–70
- [31] Yang X *et al* 2010 Multifunctional stable and pH-responsive polymer vesicles formed by heterofunctional triblock copolymer for targeted anticancer drug delivery and ultrasensitive MR imaging *ACS Nano*. **4** 6805–17